Pyrolysis of high ash sewage sludge: Kinetics and thermodynamic analysis using Coats-Redfern method

Salman Raza Naqvi [a, b, *], Rumaisa Tariq [b], Zeeshan Hameed [b], Imtiaz Ali [c], Muhammad Naqvi [d], Wei-Hsin Chen [e], Selim Ceylan [f], Harith Rashid [g], Junaid Ahmad [h], Syed A. Taqvi [i, k], Muhammad Shahbaz [j]

[a] Thermal Engineering Group, Faculty of Engineering Technology, University of Twente, 7500AE Enschede, The Netherlands
[b] School of Chemical & Materials Engineering, National University of Sciences & Technology, H-12, Islamabad, Pakistan
[c] Departments of Chemical and Materials Engineering, King Abdulaziz University, Rabigh, Saudi Arabia
[d] Department of Engineering and Chemical Sciences, Karlstad University, Sweden
[e] Department of Aeronautics and Astronautics, National Cheng Kung University, Tainan, Taiwan
[f] Ondokuz Mayıs University, Chemical Engineering Department, 55139 Samsun, Turkey
[g] Department of Chemical Engineering and Chemistry, Eindhoven University of Technology, Eindhoven, The Netherlands
[h] Faculty of Science and Technology, Free University of Bolzano, Piazza Universita 5, 39100 Bolzano, Italy
[i] Chemical Engineering Department, NED University of Engineering and Technology, 75270 Karachi, Pakistan
[j] Chemical Engineering Department, University of Gujrat, Gujrat, Pakistan
[k] Department of Chemical Engineering, Universiti Teknologi PETRONAS, Seri Iskandar, Malaysia

ARTICLE INFO

ABSTRACT

This study aims to investigate the thermo-kinetics of high-ash sewage sludge using thermogravimetric analysis. Sewage sludge was dried, pulverized and heated non-isothermally from 25 to 800 °C at different heating rates (5, 10 and 20 °C/min) in N_2 atmosphere. TG and DTG results indicate that the sewage sludge pyrolysis may be divided into three stages. Coats-Redfern integral method was applied in the 2nd and 3rd stage to estimate the activation energy and pre-exponential factor from mass loss data using five major reaction mechanisms. The low-temperature stable components (LTSC) of the sewage sludge degraded in the temperature regime of 250—450 °C while high-temperature stable components (HTSC) decomposed in the temperature range of 450—700 °C. According to the results, first-order reaction model (F1) showed higher Ea with better R^2 for all heating rates. D3, N1, and S1 produced higher Ea at higher heating rates for LTSC pyrolysis and lower Ea with the increase of heating rates for HTSC pyrolysis. All models showed positive ΔH except F1.5. Among all models, Diffusion (D1, D2, D3) and phase interfacial models (S1, S2) showed higher ΔG as compared to reaction, nucleation, and power-law models in section I and section II.

© 2018 Elsevier Ltd. All rights reserved.

1. Introduction

The growing population and rapid rate of urbanization foster potential challenges to the sustainable development [1—3]. These challenges have driven the need for treatment of valuable waste materials to clean environment [4]. The urban communities stipulate not only proper policy of municipal wastewater but also emphasize the development of suitable technology for the treatment of sewage sludge. A recent study estimated the rate of sewage sludge production to be around 0.1—30.8 kg per population equivalent per year [5,6]. The most populated country, China, is producing 20 million tons of sewage sludge through more than 3000 municipal wastewater treatment plants [7]. Solid waste management is heavily almost around 32 million tons of municipal solid waste is generated annually in Pakistan [8]. For economic development, this huge waste can be converted into bioenergy through proper waste.

The shortage of land space, rising environmental and health concern due to the presence of harmful substances such as pathogens and heavy metal in wastewater treated sewage sludge are the

* Corresponding author. Thermal Engineering Group, Faculty of Engineering Technology, University of Twente, 7500AE Enschede, the Netherlands.
E-mail addresses: s.r.naqvi@utwente.nl, salman.raza@scme.nust.edu.pk (S.R. Naqvi).

potential barriers in conventional methods of solid waste management [9,10]. Previous research reported alternative disposal techniques for sewage sludge [11,12]. However, the search to find the most appropriate method for sustainable bioenergy production from this abundant solid organic waste is ongoing. Thermochemical conversion processes gained much attention for not only handling this potential waste but also converting into renewable fuels and bioenergy [13,14]. These processes (pyrolysis, gasification, and combustion) differ based on the reactive environment and treatment temperature. Combustion identified as a mature technology in comparison to pyrolysis and gasification which is more efficient for combined heat and power production [14]. In a partial oxidative atmosphere such as gasification, the carbonaceous residue is converted into combustible gases and ash. This net reducing atmosphere can circumvent problems such as emission of sulfur and nitrogen oxides, heavy metal and fly ash which are encountered in incineration [15].

Pyrolysis is a low energy intensive and environmentally friendly process in comparison to gasification & combustion to produce gas, solid and liquid fuels with widespread applications [16]. Pyrolysis of lignocellulose biomass residues, plastic wastes, and household bio-waste are investigated in details by many researchers who exploited their useful conversion to energy and valuable chemicals [17–21]. Pyrolysis of the complex substance such as sewage sludge gained much attention recently as it provides an environmentally and economically feasible solution of biogas and bio-oil production [22,23]. To mature this technology at commercial scale, the detailed mechanism of the pyrolysis process requires knowledge of pyrolysis kinetics and process thermodynamics.

Thermogravimetric analysis has helped in estimating kinetic parameters of such complex processes [24–26]. In the analyses, major factor such as pyrolysis temperature, heating rate (slow or fast) and the role of sludge composition during decomposition were investigated [27–29]. Isoconversional methods have been used to predict the weight loss which suggested independent reactions associated with the decomposition of organic matter, non-biodegradable compounds and bacteria [32,34]. However, the investigation of pyrolysis behavior and kinetics of wastewater treated sludge is still an ongoing. Hernández et al. [30] used TGA-FTIR to study the decomposition of sewage sludge in various gases and applied multiple first-order reaction model. Friedman method was used to study the kinetics of undigested sewage sludge pyrolysis [31]. They derived reaction order which was unusually high used Coats-Redfern method to get a reasonable arbitrary reaction order to analyze the pyrolytic behavior of sludge [32]. Since sludge is a complex material therefore consideration of more extensive models is lacking in the literature. As per authors' information, a comprehensive study on pyrolysis behavior assessment, kinetics and thermodynamic parameters estimation of high ash domestic wastewater sewage sludge is lacking in literature. The Coats-Redfern integral method has been successfully utilized for the investigation of the activation energy and pre-exponential factor of complex substances [33,34]. The aim of this study is to provide knowledge on the thermal decomposition behavior, kinetics and thermodynamic potential of wastewater high-ash sewage sludge by employing five main reaction mechanisms using Coats-Redfern method.

2. Material and methodology

2.1. Sewage sludge collection and characterization

The wet sewage sludge (SS) was collected from a membrane bioreactor based wastewater treatment facility located in the National University of Sciences & Technology, Pakistan. Before pyrolysis, the sludge sample was air dried to remove the surface moisture (<10% moisture). The air-dried sewage sludge sample was crushed with mortar and pestle. The crushed sample was then ground into a fine powder, which was sieved through 1000 μm screen and stored into air-tight bags.

Proximate analysis was performed in electric oven and muffle furnace according to ASTM standard methods reported in our previous publication to find the percentage of moisture, volatile matter, fixed carbon and ash content [35]. The ultimate analysis was achieved through CHNS elementary analyzer (PerkinElmer 2400II, USA). Bomb calorimeter was used to determine high calorific value according to given ASTM standard method (D 2015, 91). Fourier Transform Infrared Spectroscopy (FTIR) analysis was performed using PerkinElmer spectrum 100 FT-IR Spectrometer to identify the functional groups present in the sewage sludge. The analysis was conducted by making pellets with KBr in 1:100 ratios. The IR scanning range was 400–4000 cm^{-1} with a resolution of 4 cm^{-1}.

2.2. Thermogravimetric analysis

The thermal degradation behavior of sewage sludge pyrolysis was determined by using thermogravimetric analyzer (TGA model no.) under nitrogen environment. The flow of nitrogen was kept at 200 ml/min with a temperature range of 25–800 °C. The initial mass of sewage sludge sample was 10±3 mg. The heating rate was 5, 10 and 20 °C/min at which the mass loss and rate of mass loss were determined with respect to temperature and time. The slow heating rate was chosen to avoid the heat transfer restrictions. To achieve the maximum accuracy and least error, experiment was repeated at least three times. The data obtained from TGA helped not only to understand the thermal decomposition behavior during pyrolysis process but also to estimate the kinetics and thermodynamic parameters of sewage sludge pyrolysis.

2.3. Kinetic study

The kinetic analysis of sewage sludge pyrolysis was simply determined by Arrhenius law, which provided information about the rate of reaction. The basic equation used for kinetic analysis of pyrolysis of sewage sludge was given below

$$\frac{d\alpha}{dt} = k(T)f(\alpha) \tag{1}$$

where

$$\alpha = \frac{m_o - m_i}{m_o - m_f} \tag{2}$$

In which m_o is initial mass, m_i is mass at given time t and m_f is final mass in mg.

$$k(T) = A \exp\left(-\frac{E_a}{RT}\right) \tag{3}$$

In which A is pre-exponential factor (min^{-1}), E_a is activation energy (kJ/mol), R is universal gas constant (0.008314 kJ/mol K) and T is reaction temperature (K).

In which n is a reaction order. For constant heating rates $\beta = \frac{dt}{dT}$, so equations (1) and (3) can be written in combined form.

$$\frac{d\alpha}{dT} = \frac{A}{\beta} \exp\left(-\frac{E_a}{RT}\right) f(\alpha) \qquad (4)$$

By applying integration to equation (5), a new equation is obtained

$$g(\alpha) = \int_0^\alpha \frac{d\alpha}{f(\alpha)} = \frac{A}{\beta} \int_{T_0}^T \exp\left(-\frac{E_a}{RT}\right) dT \qquad (5)$$

where $g(\alpha)$ is an integral form of reaction model. The analytical solution of the right side of the equation is impossible so various approximation models are used to solve the complicated part of this equation.

2.3.1. Coats-Redfern a model-fitting model

A model-fitting method, Coats-Redfern model, is extensively used to estimate the pre-exponential factor and activation energy to predict the order of reaction. The basic equation for coats and Redfern method is given below

$$\ln\left[\frac{g(\alpha)}{T^2}\right] = \ln \frac{AR}{\beta E_a}\left(1 - \frac{2RT}{E_a}\right) - \frac{E_a}{RT} \qquad (6)$$

where β is the heating rate, R is universal constant (0.008314 kJ/mol K) and $g(\alpha)$ is a kinetic function of different reaction mechanisms which is obtained from integration of $f(\alpha)$. Activation energy can be obtained by drawing a graph between $1/T$ and $\ln [g(\alpha)/T^2]$ and by obtaining slope from drawn straight line. The pre-exponential factor can be obtained from the intercept of this graph. $g(\alpha)$ can be varied according to different developed model and reaction mechanisms. Most of the solid-state degradation reactions fall in five categories which are listed below in Table 1.

2.4. Calculation of thermodynamic parameters

Thermodynamic parameters such as changes in enthalpy, Gibbs free energy and entropy can be obtained from the thermogravimetric analysis [36]. These parameters can be calculated based on kinetic data from the following equations

$$\Delta H = E_a - RT \qquad (7)$$

$$\Delta G = E_a + RT_m \ln\left(\frac{K_B T}{hA}\right) \qquad (8)$$

$$\Delta S = \frac{\Delta H - \Delta G}{T_m} \qquad (9)$$

where K_B is Boltzmann constant, which is equal to 1.381×10^{-23} m^2 kg/s^{-2} K^{-1}. T_m is maximum temperature at which

maximum decomposition occur. h is planks constant which is equal 6.626×10^{-34} m^2 kg/s and R is universal gas constant equal to 0.008314 kJ/mol K.

3. Results & discussion

3.1. Sewage sludge characterization

The air-dried sewage sludge (SS) was characterized to reveal the proximate, ultimate and high heating value (HHV). Moisture, ash, volatiles and fixed carbon of sewage sludge was 6.5 wt%, 44.6 wt%, 44.6 wt% and 4.3 wt%, respectively. The sewage sludge possessed high ash and volatile content. This high ash content and low fixed carbon leads to low heating value [37,38]. The proximate analysis results are in good agreement with previously reported articles [39]. According to ultimate analysis, sewage sludge has carbon (40.4 wt%), hydrogen (6.2 wt%), nitrogen (6.7 wt%), sulfur (1 wt%) and oxygen (45.7 wt%). It can be seen from the obtained results that sewage sludge has high carbon, oxygen and nitrogen content. Sewage sludge has high nitrogen and sulfur content as compared to biomass [37]. This high nitrogen content appears from the protein fraction of the microorganism used during wastewater purification treatment [40]. The higher heating value of sewage sludge is 11.5 MJ/kg. Thipkhunthod et al. [41] calculated the high heating value of different industrial, community and hospital sludges which were in the range of 9–13.9 MJ/kg. Fourier transform infrared (FTIR) spectroscopy is used to study the functional groups present in any substance. The FTIR spectrum of dried sewage sludge is shown in Fig. 1. This spectrum presented very extensive and wide-ranging peaks. The peak at 3428.44 cm^{-1} gives identification of hydrogen bond usually present in the O–H and N–H functional groups. The other band appeared with a sharp peak at 2921.81 cm^{-1} which is between 2880 and 3000 cm^{-1} range and represented the presence of aromatic and aliphatic groups with C–H stretching. There was another peak at around 1637.30 cm^{-1} which showed the presence
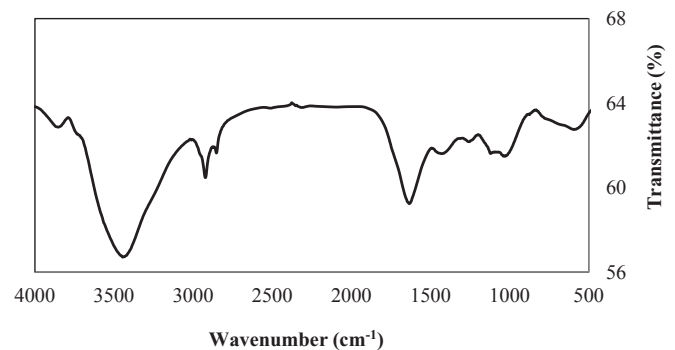

Fig. 1. FTIR spectra of sewage sludge.

Table 1
Reaction mechanisms, model names with their f(α) and g(α).

Reaction Mechanism	Model name	$f(\alpha)$	$g(\alpha)$
Chemical Reaction order	Chemical Reaction Order 1 (F1)	$1-\alpha$	$-\ln(1-\alpha)$
	Chemical Reaction Order 1.5 (F1.5)	$(1-\alpha)^{3/2}$	$2[(1-\alpha)^{-3/2}-1]$
Diffusion	Parabolic law (D1)	$1/2\alpha$	α^2
	Valensi equation (D2)	$-[\ln(1-\alpha)]^{-1}$	$\alpha + (1-\alpha)\ln(1-\alpha)$
	Ginstling-Broushtein equation (D3)	$3/2[(1-\alpha)^{1/3}-1]^{-1}$	$(1-2/3\alpha)-(1-\alpha)^{2/3}$
Nucleation and growth	Avrami-Erofeev equation Nucleation and growth (N1.5)	$3(1-\alpha)[-\ln(1-\alpha)]^{2/3}$	$[-\ln(1-\alpha)]^{2/3}$
	Avrami-Erofeev equation Nucleation and growth (N2)	$2(1-\alpha)[-\ln(1-\alpha)]^{1/2}$	$[-\ln(1-\alpha)]^{1/2}$
Phase interfacial reaction	Shrinkage geometrical column (S1)	$2(1-\alpha)^{1/2}$	$1-(1-\alpha)^{1/2}$
	Shrinkage geometrical Spherical (S2)	$3(1-\alpha)^{2/3}$	$1-(1-\alpha)^{1/3}$
Power law	Power law (P)	1	α

of C=O aldehyde group. The section between 1550 and 1350 cm^{-1} could be appeared due to the vibrations of CH$_2$ and CH$_3$ groups. A strong peak was also detected at 1000 cm^{-1} which could be due to stretching vibrations of the C−O and C−O−C groups. This peak showed the presence of alcohol, ethers, esters and carboxylic acid due to the presence of oxygen. Below 1000 cm^{-1} data interpretation became difficult because of skeletal vibrations. Dominguez et al. [41] also performed FTIR of dried sewage sludge and confirmed the presence of N−H, O−H, C−H, CH$_2$, CH$_3$, C=O functional group by assigning peaks at given range of wavenumber.

3.2. Thermal degradation behavior of SS

Fig. 2 represented three mass loss curves with respect to temperature at three different heating rates of 5, 10 and 20 °C/min. These three curves were mainly divided into three stages. Stage one was mainly ascribed to the loss of surface and free bound water between 70 and 150 °C. The second stage showed significant mass loss between the temperature ranges of 200−600 °C. Initially between 200 and 370 °C, thermal decomposition reactions were observed and involved decomposition of biodegradable materials such as hydrocarbons. The decomposition of organic matter such as protein, sugars, and aliphatic compounds was observed between the temperature ranges of 400−600 °C, which is main and active pyrolysis zone [35]. The third range, above 600 °C, showed the thermal degradation of inorganic contents such as calcium carbonate. Other authors presented similar trends and observations [33,42].

Table 2 listed TG-DTG data at 5, 10 and 20 °C/min which provided characteristic pyrolysis temperature and percentage mass loss. As mentioned above the main thermal degradation range was from 200 °C to 600 °C which was further separated into two ranges. In first range, initial temperature (T$_i$) where sludge degradation appeared at 300 °C for 5 °C/min, 315 °C for 10 °C/min and 330 °C for 20 °C/min. Final temperature (T$_f$) and maximum peak temperature (T$_p$) in first range for 5, 10 and 20 °C/min were 400 & 350, 430 &

380, and 440 & 400 °C), respectively. In second range, T$_i$, T$_f$, and T$_p$ were appeared at the heating rates of 5 °C/min (500, 610 and 540 °C), at 10 °C/min (510, 630 and 555 °C) and at 20 °C/min (530, 660 and 575 °C), respectively. The intensification of heating rate subsidies to the rapid thermal degradation processes towards elevated temperatures, this fact could be enlightened that a high heating rate of sewage sludge sample with respect to given temperature in a short time as a result of the increased thermal delay. Secondly, the higher amount of volatile matter released to some extent with increasing heating rate.

3.3. Kinetic analysis of sewage sludge pyrolysis

After illustrating the pyrolysis process of sewage sludge sample, various types of kinetic models with the different kinetic mechanism of pyrolysis could be further acknowledged on the basis of thermal decomposition study. Representative mechanism functions were used to satisfy these results, as represented in Table 3. The appropriate model can be chosen on the basis of linear fitting of the main solid-state reaction kinetic models and the linear regression coefficient R^2 of each model. The model with the linear regression R^2 nearly equal to 0.99 could be considered as the most appropriate mechanism model. However, this is not hard and fast rule. The value of R^2 would not provide assurance that the selected reaction mechanism of pyrolysis process was best fitted or not. For kinetic analysis of sewage sludge, the Coats-Redfern model was used to determine the activation energy (Ea, kJ/mol) and pre-exponential factor (A, min^{-1}).

Table 3 listed the activation energy, regression coefficient and pre-exponential factor for two pyrolysis zones (section I: 240−330 °C & section II: 400−550 °C). The kinetic parameters were calculated at heating rates of 5, 10 and 20 °C/min by employing various reaction models. All given model provided linear regression coefficient R^2 from 0.91 to 0.99 except at 10 °C/min for power law (P) at temperature range of section I from 240 to 330 °C and 5 °C/min for Avrami-Erofeev equation (Nucleation and growth, N2) at temperature range of section II at 400−550 °C which showed poor linear regression like 0.89 and 0.85 for both models. Phase interfacial reaction shrinkage geometrical column (S1) model at 10 °C/min could be considered as best fitted model based on ideal linear regression equal to 0.99 for both sections. In chemical reaction models, first order showed higher activation energy (25.8, 29.3 and 27.4 kJ/mol for section I and 9.61, 1.31 and 1.21 kJ/mol for section II) at 5, 10, and 20 °C/min with better regression coefficient. In diffusion models, with increasing heating rates D3 showed lower activation energy in section I and higher activation energy in section II at higher regression coefficient (R^2~0.99) in comparison to D1 and D2. In a similar manner of comparison, N1 and S1 produced higher activation energy at higher heating rates in section I and lower activation energy with the increase of heating rates in section II with the better linear plot. Power law (P) showed very low activation energy in section I in comparison to first order reaction, diffusion, nucleation and phase interfacial reaction models with

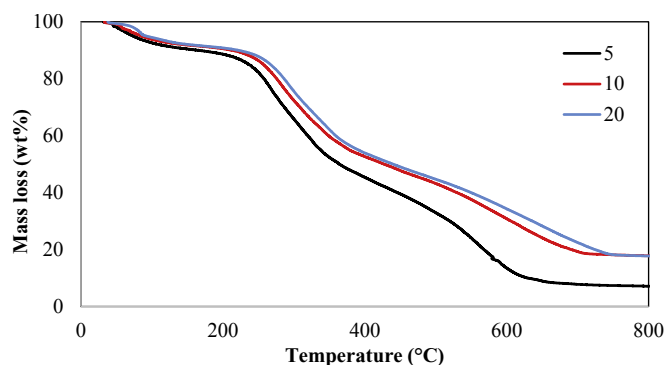**Fig. 2.** TGA of sewage sludge sample at 5, 10 and 20 °C/min.

Table 2
TG-DTG characteristics parameters of sewage sludge at heating rates of 5, 10 and 20 °C/min.

Heating rates (°C/min)	Range I (250−450 °C)				Range II (450−700 °C)			
	Ti (°C)	Tf (°C)	Tp (°C)	DTG (s^{-1})	Ti (°C)	Tf (°C)	Tp (°C)	DTG (s^{-1})
5	300	400	350	0.00050	500	610	540	0.00060
10	315	430	380	0.00055	510	630	555	0.00065
20	330	440	400	0.00150	530	660	575	0.00125

T$_i$ = Initial temperature where degradation starts, T$_f$ = Final temperature.
T$_p$ = Maximum peak temperature.

Table 3
Kinetic parameters of sewage sludge sample by using various reaction models at heating rates of 5, 10 and 20 °C/min.

Model Name	Heating Rates (°C/min)	Section I (240—330 °C)			Section II (400—550 °C)		
		E_a (kJ/mol)	R^2	A (min^{-1})	E_a (kJ/mol)	R^2	A (min^{-1})
F1	5	25.80	0.985	47.55	9.61	0.988	44.99
	10	29.34	0.994	95.28	1.31	0.942	156.66
	20	27.4	0.979	206.96	1.21	0.982	280.00
F1.5	5	0.03	0.963	47.50	0.06	0.997	78.33
	10	0.03	0.967	95.00	1.31	0.998	156.60
	20	0.04	0.975	206.66	3.63	0.996	280.00
D1	5	48.92	0.981	52.71	10.90	0.987	44.99
	10	56.28	0.992	144.18	2.73	0.992	89.99
	20	54.64	0.986	259.37	3.49	0.977	159.98
D2	5	52.62	0.992	55.15	16.34	0.984	78.33
	10	59.90	0.993	159.08	6.02	0.996	156.67
	20	57.60	0.985	264.53	6.52	0.995	280.00
D3	5	12.13	0.997	47.48	19.60	0.999	78.33
	10	11.75	0.995	94.99	16.73	0.999	156.66
	20	10.97	0.994	206.62	15.99	0.999	280.00
N1.5	5	14.09	0.976	47.45	2.24	0.915	78.33
	10	16.45	0.991	95.01	3.28	0.996	156.66
	20	15.20	0.971	206.00	3.25	0.997	280.00
N2	5	8.27	0.961	47.49	9.64	0.852	83.40
	10	10.04	0.986	94.99	5.56	0.999	89.99
	20	15.7	0.945	206.65	1.21	0.981	280.00
S1	5	22.71	0.978	47.49	3.82	0.959	78.38
	10	26.33	0.991	95.06	2.10	0.992	156.66
	20	25.02	0.98	206.75	1.82	0.975	280.00
S2	5	23.72	0.981	47.51	5.61	0.977	78.38
	10	27.32	0.992	95.05	1.03	0.955	156.67
	20	25.81	0.979	206.73	0.87	0.926	280.00
P	5	5.29	0.893	47.49	6.60	0.997	78.33
	10	7.13	0.965	94.99	8.65	0.999	156.67
	20	6.78	0.952	206.66	8.24	0.998	280.00

poor linearity. However, in section II, P showed higher activation energy than S2, S1, N2, N1, F1.5, and F1.

Pre-exponential factor increased as the heating rate increased as illustrated in Table 3. Pre-exponential factor at 20 °C/min was 280 min^{-1} for almost every model in section II and was 206 min^{-1} for almost all models in section I. Usually A is related to the number of times molecules will hit in the orientation necessary to cause a reaction [43]. The calculated range of pre-exponential factor for each model was 47—206 min^{-1} for temperature range 240—330 °C and 44-280 min^{-1} for temperature range 400—550 °C. Zhang et al. [44] predicted Ea and A values as 18.03 kJ/mol and 1391 min^{-1} for the first mass loss range and 11.87 kJ/mol and 111 min^{-1} for the second mass loss range, respectively for sewage sludge sample obtained from the municipal wastewater treatment plant.

3.4. Thermodynamic parameters calculation

Thermodynamic parameters such as change in enthalpy (ΔH kJ/mol), change in Gibbs free energy (ΔG, kJ/mol) and change in entropy (ΔS, kJ/mol K) were calculated at 5, 10 and 20 °C/min by using different type of reaction mechanism models as shown in Table 4. ΔH, which is a state function, reflected the absorbed or released heat at constant pressure [45]. All models showed positive ΔH except F1.5 in section I. The positive ΔH indicated that energy from an external source is needed for the higher energy level of the reagents to their transition state [46]. A growth in the ΔH value, time for total conversion of sewage sludge pyrolysis also increased. Thus, a higher value of the change in enthalpy could alter the activity of primary reaction in pyrolysis [47]. ΔH followed the similar pattern as activation energy increased with the increasing heating rates. ΔG revealed the total increase energy in approach of the reagents and the formation of the activated complex [48]. This provides a

comprehensive approach to evaluate the disorder & heat flow change and its higher value represents a lower favorability of reaction [36]. Among all models, diffusion (D1, D2, D3) and phase interfacial models (S1, S2) showed higher ΔG as compared to reaction, nucleation, and power-law models in section I and section II. The value of ΔG decreased with the with the increase of heating rates in section II for all models which facilities the pyrolysis process of sewage sludge at higher temperatures (400—550 °C).

The ΔS in Table 4 showed negative values which confirmed the disorder of products resulted through bond dissociation was lower than initial reactants. These negative values represented that the disintegration in the activated state has a more well-organized structure than before the thermal disintegration and that the reactions in the activated state are gentler than anticipated. The ΔS from sewage sludge at various heating rates varied from −181 J/mol to −225 J/mol which is higher than rice straw and rice bran, −4.13 J/mol and −62 J/mol, respectively [49].

4. Conclusions

In this study, thermo-kinetic and thermodynamic parameters of sewage sludge were systematically investigated. The thermal analysis of TG and DTG data indicated sewage sludge pyrolysis as a multi-step process with complex reaction mechanisms. Heating rate was found to affect mass loss and mass loss rates, significantly. Thermo-kinetic analysis was performed using Coats-Redfern method on two thermal regimes; low-temperature stable (LTS) and high-temperature stable (HTS). In every model, activation energy decreased at elevated temperature zone that means that reaction rate constant increased and speed-up the reactions occurring during the pyrolysis process. Higher correlation coefficient suggested best suitable model for the description of complex

Table 4
Thermodynamic parameter estimation of sewage sludge at heating rates of 5, 10 and 20 °C/min.

Model Name	Heating Rate (°C/min)	Section I (240–330 °C)			Section II (400–550 °C)		
		ΔH (kJ/mol)	ΔG (kJ/mol)	ΔS (kJ/mol.K)	ΔH (kJ/mol)	ΔG (kJ/mol)	ΔS (kJ/mol.K)
F1	5	23.43	86.342	−0.2207	5.702	111.623	−0.2253
	10	26.97	88.235	−0.2149	−2.597	98.448	−0.2149
	20	24.80	89.679	−0.2092	−2.282	85.593	−0.2092
F1.5	5	−2.33	60.575	−0.2207	−3.901	99.852	−0.2207
	10	−2.33	58.938	−0.2149	−2.595	98.452	−0.2149
	20	−2.54	62.325	−0.2092	0.1446	88.020	−0.2092
D1	5	46.55	109.218	−0.2198	6.99	112.913	−0.2253
	10	53.91	114.194	−0.2115	0.485	102.034	−0.2160
	20	52.06	116.337	−0.2073	−0.00188	89.828	−0.2138
D2	5	50.25	122.811	−0.2546	12.432	116.186	−0.2207
	10	57.53	117.581	−0.2107	2.1169	103.162	−0.2149
	20	55.02	119.247	−0.2072	3.0281	90.903	−0.2092
D3	5	9.76	72.676	−0.2207	15.69	119.446	−0.2207
	10	9.38	70.653	−0.2149	12.082	113.868	−0.2165
	20	8.39	73.253	−0.2092	12.498	100.373	−0.2092
N1.5	5	11.72	74.637	−0.2207	−1.487	102.086	−0.2203
	10	14.08	75.352	−0.2149	−0.6275	100.418	−0.2149
	20	12.62	77.491	−0.2092	−0.2418	87.633	−0.2092
N2	5	5.90	68.815	−0.2207	92.49	178.006	−0.1819
	10	7.67	68.943	−0.2149	1.652	104.864	−0.2196
	20	13.12	77.983	−0.2092	−2.2818	85.593	−0.2092
S1	5	20.34	83.255	−0.2207	−0.08758	103.664	−0.2207
	10	23.96	85.231	−0.2149	−1.8075	99.283	−0.2150
	20	22.44	87.302	−0.2092	−1.6718	86.203	−0.2092
S2	5	21.35	84.264	−0.2207	1.7024	105.454	−0.2207
	10	24.95	86.221	−0.2149	−2.8685	98.176	−0.2149
	20	23.23	88.092	−0.2092	−2.6218	85.253	−0.2092
P	5	2.92	65.853	−0.2208	2.692	106.446	−0.2207
	10	4.76	66.033	−0.2149	4.742	105.787	−0.2149
	20	4.20	69.063	−0.2092	4.7481	92.623	−0.2092

and high ash sewage sludge pyrolysis process. Kinetic and thermodynamic parameters information will be vital and useful knowledge for large-scale sewage sludge pyrolysis process for bioenergy application.

Acknowledgment

References

[1] S.R. Naqvi, et al., Potential of biomass for bioenergy in Pakistan based on present case and future perspectives, Renew. Sustain. Energy Rev. 81 (Part 1) (2018) 1247–1258.

[2] V. Dhyani, T. Bhaskar, A comprehensive review on the pyrolysis of lignocellulosic biomass, Renew. Energy 129 (Part B) (December 2018) 695–716.

[3] W. Won, C.T. Maravelias, Thermal fractionation and catalytic upgrading of lignocellulosic biomass to biofuels: process synthesis and analysis, Renew. Energy 114 (2017) 357–366.

[4] E. Toklu, Biomass energy potential and utilization in Turkey, Renew. Energy 107 (2017) 235–244.

[5] A. Kelessidis, A.S. Stasinakis, Comparative study of the methods used for treatment and final disposal of sewage sludge in European countries, Waste Manag. 32 (6) (2012) 1186–1195.

[6] J. Peccia, P. Westerhoff, We should expect more out of our sewage sludge, Environ. Sci. Technol. 49 (14) (2015) 8271–8276.

[7] G. Yang, G. Zhang, H. Wang, Current state of sludge production, management, treatment and disposal in China, Water Res. 78 (Supplement C) (2015) 60–73.

[8] M.S. Korai, R.B. Mahar, M.A. Uqaili, The feasibility of municipal solid waste for energy generation and its existing management practices in Pakistan, Renew. Sustain. Energy Rev. 72 (Supplement C) (2017) 338–353.

[9] H.-j. Huang, et al., Co-pyrolysis of sewage sludge and sawdust/rice straw for the production of biochar, J. Anal. Appl. Pyrol. 125 (2017) 61–68.

[10] M. Paneque, et al., Hydrothermal carbonization and pyrolysis of sewage sludges: what happen to carbon and nitrogen? J. Anal. Appl. Pyrol. 128 (2017) 314–323.

[11] D. Fytili, A. Zabaniotou, Utilization of sewage sludge in EU application of old and new methods—a review, Renew. Sustain. Energy Rev. 12 (1) (2008) 116–140.

[12] W. Rulkens, Sewage sludge as a biomass resource for the production of energy: overview and assessment of the various options, Energy Fuels 22 (1) (2008) 9–15.

[13] P. Stasta, et al., Thermal processing of sewage sludge, Appl. Therm. Eng. 26 (13) (2006) 1420–1426.

[14] P. Manara, A. Zabaniotou, Towards sewage sludge based biofuels via thermochemical conversion—a review, Renew. Sustain. Energy Rev. 16 (5) (2012) 2566–2582.

[15] T.W. Marrero, et al., Fate of heavy metals and radioactive metals in gasification of sewage sludge, Waste Manag. 24 (2) (2004) 193–198.

[16] J. Jin, et al., Influence of pyrolysis temperature on properties and environmental safety of heavy metals in biochars derived from municipal sewage sludge, J. Hazard Mater. 320 (2016) 417–426.

[17] S. Wang, et al., Lignocellulosic biomass pyrolysis mechanism: a state-of-the-art review, Prog. Energy Combust. Sci. 62 (Supplement C) (2017) 33–86.

[18] W. Chen, et al., Investigation on biomass nitrogen-enriched pyrolysis: influence of temperature, Bioresour. Technol. 249 (Supplement C) (2018) 247–253.

[19] S.R. Naqvi, M. Naqvi, Catalytic fast pyrolysis of rice husk: influence of commercial and synthesized microporous zeolites on deoxygenation of biomass pyrolysis vapors, Int. J. Energy Res. 42 (3) (10 March 2018) 1352–1362.

[20] S.D. Anuar Sharuddin, et al., A review on pyrolysis of plastic wastes, Energy Convers. Manag. 115 (Supplement C) (2016) 308–326.

[21] S. Vakalis, et al., Thermochemical valorization and characterization of household biowaste, J. Environ. Manag. 203 (Part 2) (2017) 648–654.

[22] S. Luo, et al., Effect of particle size on pyrolysis of single-component municipal solid waste in fixed bed reactor, Int. J. Hydrogen Energy 35 (1) (2010) 93–97.

[23] J. Alvarez, et al., Characterization of the bio-oil obtained by fast pyrolysis of sewage sludge in a conical spouted bed reactor, Fuel Process. Technol. 149 (Supplement C) (2016) 169–175.

[24] G. Liu, H. Song, J. Wu, Thermogravimetric study and kinetic analysis of dried industrial sludge pyrolysis, Waste Manag. 41 (2015) 128–133.

[25] Y. Zhai, et al., Pyrolysis characteristics and kinetics of sewage sludge for different sizes and heating rates, J. Therm. Anal. Calorim. 107 (3) (2012) 1015–1022.

[26] J.A. Conesa, et al., Kinetic study of the pyrolysis of sewage sludge, Waste Manag. Res. 15 (3) (1997) 293–305.

[27] L.F. Calvo, et al., Heating process characteristics and kinetics of sewage sludge in different atmospheres, Thermochim. Acta 409 (2) (2004) 127–135.

[28] Z. Wang, et al., Low temperature pyrolysis characteristics of oil sludge under various heating conditions, Energy Fuels 21 (2) (2007) 957–962.

[29] X. Huang, et al., Influences of pyrolysis conditions in the production and chemical composition of the bio-oils from fast pyrolysis of sewage sludge,

J. Anal. Appl. Pyrol. 110 (1) (2014) 353—362.

[30] A.B. Hernández, F. Okonta, N. Freeman, Thermal decomposition of sewage sludge under N2, CO2 and air: gas characterization and kinetic analysis, J. Environ. Manag. 196 (Supplement C) (2017) 560—568.

[31] J.A. Consea, et al., Kinetic model for the continuous pyrolysis of two types of polyethylene in a fluidized bed reactor, J. Anal. Appl. Pyrol. 40 (41) (1997) 419—431.

[32] J. Shao, et al., Pyrolysis characteristics and kinetics of sewage sludge by thermogravimetry fourier transform infrared analysis, Energy Fuels 22 (1) (2008) 38—45.

[33] J. Hu, et al., Effectiveness of wind turbine blades waste combined with the sewage sludge for enriched carbon preparation through the co-pyrolysis processes, J. Clean. Prod. 174 (Supplement C) (2018) 780—787.

[34] K. Jayaraman, M.V. Kok, I. Gokalp, Thermogravimetric and mass spectrometric (TG-MS) analysis and kinetics of coal-biomass blends, Renew. Energy 101 (Supplement C) (2017) 293—300.

[35] S.R. Naqvi, et al., In situ catalytic fast pyrolysis of paddy husk pyrolysis vapors over MCM-22 and ITQ-2 zeolites, J. Anal. Appl. Pyrol. 114 (2015) 32—39.

[36] Y.S. Kim, Y.S. Kim, S.H. Kim, Investigation of thermodynamic parameters in the thermal decomposition of plastic waste-waste lube oil compounds, Environ. Sci. Technol. 44 (13) (2010) 5313—5317.

[37] M. Tomasi Morgano, et al., Screw pyrolysis technology for sewage sludge treatment, Waste Manag. 73 (March 2018) 487—495.

[38] M. Atienza-Martínez, et al., Fast pyrolysis of torrefied sewage sludge in a fluidized bed reactor, Chem. Eng. J. 259 (Supplement C) (2015) 467—480.

[39] E. Agrafioti, et al., Biochar production by sewage sludge pyrolysis, J. Anal. Appl. Pyrol. 101 (Supplement C) (2013) 72—78.

[40] I. Fonts, et al., Sewage sludge pyrolysis for liquid production: a review, Renew.

Sustain. Energy Rev. 16 (5) (2012) 2781—2805.

[41] A. Domínguez, et al., Production of bio-fuels by high temperature pyrolysis of sewage sludge using conventional and microwave heating, Bioresour. Technol. 97 (10) (2006) 1185—1193.

[42] X. Wang, et al., Synergetic effect of sewage sludge and biomass co-pyrolysis: a combined study in thermogravimetric analyzer and a fixed bed reactor, Energy Convers. Manag. 118 (Supplement C) (2016) 399—405.

[43] V. Balasundram, et al., Thermogravimetric catalytic pyrolysis and kinetic studies of coconut copra and rice husk for possible maximum production of pyrolysis oil, J. Clean. Prod. 167 (Supplement C) (2017) 218—228.

[44] X.Y. Zhang, M.Q. Chen, A comparison of isothermal with nonisothermal drying kinetics of municipal sewage sludge, J. Therm. Anal. Calorim. 123 (1) (2016) 665—673.

[45] H. Li, et al., Comparative evaluation of thermal degradation for biodiesels derived from various feedstocks through transesterification, Energy Convers. Manag. 98 (Supplement C) (2015) 81—88.

[46] L. Huang, et al., Thermodynamics and kinetics parameters of co-combustion between sewage sludge and water hyacinth in CO2/O2 atmosphere as biomass to solid biofuel, Bioresour. Technol. 218 (Supplement C) (2016) 631—642.

[47] B.V. Babu, A.S. Chaurasia, Parametric study of thermal and thermodynamic properties on pyrolysis of biomass in thermally thick regime, Energy Convers. Manag. 45 (1) (2004) 53—72.

[48] S.C. Turmanova, et al., Non-isothermal degradation kinetics of filled with rise husk ash polypropene composites, Express Polym. Lett. 2 (2) (2008) 133—146.

[49] A.A.D. Maia, L.C. de Morais, Kinetic parameters of red pepper waste as biomass to solid biofuel, Bioresour. Technol. 204 (Supplement C) (2016) 157—163.